Asian Journal of Chemistry; Vol. 27, No. 11 (2015), 3930-3936

ASIAN JOURNAL OF CHEMISTRY

http://dx.doi.org/10.14233/ajchem.2015.18895

Effect of Synthesis and Photocatalytic Activities of Metal Oxide in Degradation of Phenol in Organic Contaminants

I. PRABHA

Department of Chemistry, Sathyabama University, Chennai-600 116, India

Corresponding author: E-mail: ipsathyabama@gmail.com

Received: 2 December 2014; *Accepted*: 27 January 2015; *Published online*: 16 July 2015; AJC-17378

The present study involves synthesis, characterization and application of ZnO nanoparticles for the photodegradation of phenol in wastewater. Zinc oxide nanoparticles were synthesized by sol-gel process calcination at 500 °C. The characterization was done by X-ray diffraction, scanning electron microscope and Brunauer-Emmet-Teller method to analyze the crystallite size, particle size, surface area. The crystallite size of ZnO nanoparticles was found to be comprised of 25-35 nm and the particle size was confirmed as 30 ± 5 nm with heterogeneous and spherical in shape. The photocatalytic activity of ZnO nanoparticles was evaluated using phenol as a model pollutant in UV and solar light. The photocatalytic experiments were carried out in a batch mode using 8 W UV lamp which emits a peak wavelength of 254 nm. The intensity of the sunlight during the reaction time was in the range of 808-1070 W/m^2. Under optimum condition, ZnO nanoparticles showed higher degradation. A series of experiments were conducted to investigate the effect of concentration and effect of catalyst loading. The photocatalytic process follows pseudo first order kinetics. The addition of H_2O_2 leads to better enhancement for the degradation of organic contaminants in the presence of ZnO nanoparticles. The reusability of the ZnO nanoparticles has also been investigated.

Keywords: Textile wastewater, Degradation, Organic contaminants, Nanoparticles, Photocatalyst.

INTRODUCTION

Large amount of organic wastewater generated from industrial processes, such as plating, machining, fertilizer, cosmetic, paint productions, food-processing *etc.*, consisting of emulsions are complex and are difficult to treat[1]. Generally, there are processes are in practice to treat the wastewater such as skimming, emulsion breaking, dissolved-air flotation, gravity separation and chemical demulsification. But most of these have drawbacks and are only partly effective[2]. As international environmental standards are becoming more strict for the development of technological systems for the removal (or degradation/ toxic into non-toxic forms) of organic pollutants such as phenolic compounds have been recently on rise. The system include physical methods (*e.g.* adsorption)[3], biological methods (*e.g.* biodegradation)[4] and chemical methods (*e.g.* chlorination, ozonation)[5]. But these methods are non-destructive, less feasible, they only transfer the non-biodegradable matter into sludge, giving rise to new type of pollution, which needs further treatment of solid-wastes and regeneration of the adsorbent which will add more cost to the process and thus chances for better method are still well open[6,7]. Hence there is a need to develop treatments methods that are more effective in eliminating organic pollutants from the wastewater[8].

Photocatalytic degradation process as extensively applied to organic contamination treatment because it is effective, eco-friendly, low cost and rapid technique for the complete removal of pollutants from wastewater[9]. Heterogeneous photocatalysis has been emerged as an efficient method for purification of water and air[10-12]. In most cases, the effective materials for photocatalytic applications are nano-sized semiconductor oxide (ZnO), which has been proven as excellent catalyst because of its highly reactive surfaces[13]. Zinc oxide nanoparticles have been extensively examined as heterogeneous semiconductor photocatalyst because of their high capacity for degradation of toxic and recalcitrant chemical species *via* relatively simple and low-cost procedure[14,15]. Nanosized ZnO has been chosen as one of the photocatalysts[16] due to its direct energy gap of about 3.3 eV, large volume to area ratio, high ultraviolet (UV) absorption and long life-span[17], gas sensor[18], active filler for rubber and plastic, UV absorber in cosmetics and anti-virus agent in coating[19] and it absorbs UV radiation due to the band-to-band transitions[20]. Also nano ZnO has attracted and growing attention due to its potential applications, in ultraviolet light emitting devices and laser devices. Now-a-days utilization of solar light becomes an appealing challenge for developing photocatalysis because of its efficiency, low cost and environmental friendly.

Nanometer-sized particles have very different physical and chemical properties from bulk materials. Also their catalytic activity is expected to be enhanced due to their increased surface area and the changes of surface properties such as surface defects. In the presence of ZnO nanoparticles, the photocatalytic process usually involves following steps: (1) Adsorption of the organic pollutant (2) Photogenerated electrons in the conduction band, which are trapped by a recipient (such as oxygen) to give superoxide radicals (3) Photogenerated holes in the valence band are consumed by donors (such as phenol organics) or sometimes by OH^- to generate $OH^\bullet$ radicals (4) The reaction of highly reactive radicals with the adsorbed phenol to give degraded product(s). This finally results in desorption of the product(s) from the interface region to make the water less toxic[21]. The higher the mobility of the photogene-rated carriers (including holes and electrons), the better is the performance of the photocatalyst. Additionally, the valence band position of a semiconductor and the incident photon energy also plays an important role in deciding the photo-catalytic activity of the semiconductor. The deeper the valence band of a semiconductor, the stronger is its oxidative activity and higher is the photo-catalytic property of the material[22,23].

In the present work, the suitability of ZnO nanoparticles for degrading common organic contaminants such as phenol was tested. Zinc oxide nanoparticles were prepared and characterized by XRD, SEM and BET surface area analysis methods. The photodegradability of ZnO nanoparticles was investigated under UV and solar light. The effective parameters such as catalyst loading and concentration of phenol solution have been studied. The efficiency of the catalytic activity showed dependence on particle size, crystallinity and surface area. A complete cleanup of a synthetic organic cocktail in water was effectively achieved using the ZnO nanoparticles. Hence, ZnO nanoparticles can serve as a good photocatalyst to identify and cleanup a variety of common organic contaminants found in wastewater using UV light irradiation and solar light.

EXPERIMENTAL

Zinc acetate dihydrate, oxalic acid dihydrate and ethanol and all the organic reagents were analytical grade purchased from Merck, Qualigens, India. The estimation of phenol was done spectrophotometrically using 4-amino antipyrine method[24]. Solutions have been prepared using double distilled water was used for all the measurements.

Synthesis of ZnO nanoparticles: The ZnO nanoparticles were synthesized by sol-gel method with some changes[25]. In this experiment, 10.98 g of zinc acetate dihydrate was treated with 300 mL of ethanol in an oil bath at 60 ºC on magnetic stirrer with medium rotation. The ethanol in zinc acetate solution was stirred continuously for 1.5 h until it becomes transparent. Simultaneously 12.6 g of oxalic acid dihydrate was dissolved in 200 mL of ethanol on constant stirring at 50 ºC for 5-10 min on magnetic stirrer with medium rotation. Next oxalic acid in ethanol was added drop wise to the warm ethanolic solution containing Zn^{2+} drop wise with continuous stirring and maintained this sample on magnetic stirrer for 45 min for complete mixing. After this the thick white gel of zinc oxide obtained was dried in a vacuum oven at 80 ºC for 20 h to get xerogel. It was calcined at 500 ºC at a ramp rate of 3 ºC/min for 5 h to yield ZnO nanoparticles.

Analytical techniques and procedures: The XRD analysis was done to analyze the crystallite size of ZnO nanoparticles. Sample for powder X-ray Diffraction was prepared by making a thin film of powder with ethanol on a glass plate and the measurement was performed with a Rigaku Geigerflex X-ray diffractometer with Ni-filtered CuK_α radiation (λ = 1.5418 Å, 30 kV, 15 mA). The XRD patterns were recorded in the range of 10-60°, with a scan speed of 2°/min and X-ray source operating voltage of 40 kv. The average crystallite size was determined according to the Scherrer equation using the full width at half maximum (FWHM) data of the phase after correcting the instrumental broadening. The particle size and morphology of ZnO nanoparticles was observed using scanning electron microscopy (SEM) using FESEM-SUPRA55, CARL ZEISS, Germany was used in the experiments. The surface area (BET method) of the sample was determined from nitrogen adsorption-desorption isotherms at liquid nitrogen temperature using a Micrometrics ASAP 2020 automated system with outgas for 15 min at 150 °C.

Experimental set up: The photodegradation studies have been carried out in a batch reactor system. The slurry is stirred magnetically and low-pressure mercury vapour lamp has been used as an irradiation source. The lamp emits 8 W of UV radiation with a peak wavelength of 254 nm. The reactor configuration and operating conditions for the photocatalytic degradation have been optimized by preliminary trial experiments with respect to (i) the total batch volume of reactant solution, (ii) the stirring speed and (iii) the time for adsorption equilibrium prior to exposure to UV light. The optimum condition consists of a batch volume of 250 mL, stirring speed of 70 rpm and 0.5 h for adsorption equilibrium. The experimental procedure consists of irradiation of the phenol solution of known concentration mixed with a known weight of catalyst powder at a constant volume of 250 mL. The slurry has been stirred well using a magnetic stirrer throughout the period of experiment. In all the studies the suspensions have been stirred well for about 0.5 h to allow equilibration of adsorption process before exposure to UV light. Samples of 3 mL have been withdrawn at regular intervals of time, centrifuged, absorbance measured at 500 nm, respectively and returned to the reactor. All studies have been carried out at 30 ºC at pH = 7.

Reactor setup and procedures for solar experiments have been similar to photocatalysis mediated by UV light. The solutions have been illuminated in an open rectangular tray made from borosilicate glass. The slurry was mixed with the definite weight and stirred for 0.5 h in the dark prior to illumination in order to achieve maximum adsorption of phenol onto the semiconductor surface. During the illumination time no volatility of the solvent was observed. The temperature has been monitored and the evaporation losses have been calculated. The photodegradation study has been carried out in direct sunlight under optimum condition. Sun light intensity was measured for every 0.5 h and the average light intensity over the duration of each experiment was calculated. The intensity of the sunlight during the reaction time was in the range of 808-1070 W/m^2. The intensity was nearly constant during the experiments.

RESULTS AND DISCUSSION

X-ray diffraction study: X-ray diffraction measurement was employed to investigate the phase and structure of the synthesized ZnO nanoparticles. It was obtained by the thermal treatment of the precursors at 500 °C under air atmosphere is shown in Fig. 1. The XRD peaks correspond to the (100), (002), (101), (102), (110), (103), (200), (112) and (201) planes of ZnO nanoparticles and it can be seen that all these peaks are in good agreement with wurtzite ZnO (a = 0.3249 nm and c = 0.52 nm) and the obtained spectrum has the first ZnO main peaks at 2θ = 31.7,34.4, 36.2, 47.5, 56.5, 62.8, 66.4, 67.9 and 69.8 which is in exact agreement with the 36-1451 standard card from the Joint Committee for Powder Diffraction Studies (JCPDS). No impurities are observed, which indicates high purity, crystallinity and ultra fine nature of the crystallites of the as-obtained Wurtzite ZnO nanoparticles. So the thermal treatment of these precursors under air atmosphere can bring about the conversion of zinc acetate to ZnO nanoparticles. The average crystallite size obtained with calcination temperature at 500 ºC is estimated to be 30 ± 5 nm by applying the Debye-Sherrer formula. The calcinating temperature (at 500 ºC) provides energy of atoms to enhance mobility that could decrease the structural defects and improve the crystalline degree. This was confirmed using scanning electron microscopy (Fig. 2), which revealed that the material consisted of agglomerates of hexagonal wurtzite structure whereas the electron microscopy can be used to determine almost any crystallite size.

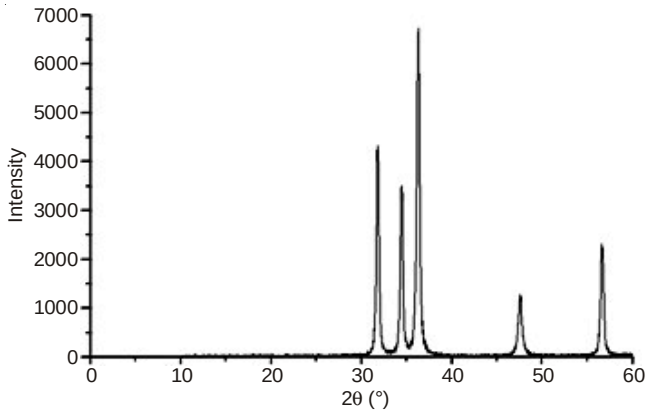

Fig. 1. X-ray powder diffraction plot of ZnO nanoparticles

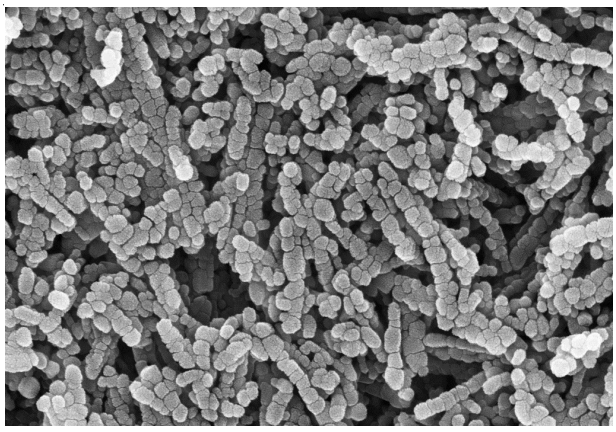

Fig. 2. SEM micrograph of ZnO nanoparticles 500 ºC

SEM micrograph of ZnO nanoparticles: Shape and morphology is clearly observed in the SEM micrograph of the ZnO nanoparticles. Fig. 2 shows the SEM micrograph of prepared ZnO nanoparticles which revealed the particles are grown in a very high-density due to the concentration of zinc ions has a certain impact on the particle size and distribution of ZnO nanoparticles that showed the particle size was around 35 ± 5 nm and the average particle size was found to be 30.26 nm. It shows heterogeneous particles are spherical shape in nature which are coherent with each other. It can be seen that the concentration of Zn^{2+} has a certain impact on the particle size and distribution of ZnO nanoparticles. Also the calcinating temperature (500 °C) has noticeable effect on the particle size and morphology of the ZnO nanoparticles. It indicates that activation energy barrier for the formation of well-dispersed ZnO nanoparticles could not be overcome. Surface area of ZnO is analyzed by using BET analysis and the surface area of ZnO nanoparticles is found to be 11.09 m^2/g. From this it is concluded that surface area of ZnO nanoparticles decrease with the increase in ZnO content. Table-1 shows the crystallite size, particle size, morphology and surface area of the ZnO nanoparticles.

TABLE-1
CRYSTALLITE SIZE, PARTICLE SIZE AND SURFACE AREA OF THE ZnO NANOPARTICLES

Nanophotocatalyst	ZnO
Crystallite size (nm)	25-35
Particle size (nm)	35 ± 5
Morphology	Spherical in shape which are coherent together
Surface area (m^2/g)	11.09

Photodegradability of ZnO nanoparticles: The photodegradability of the phenol solution has been investigated by exposing the phenol solution to UV light in the absence and in the presence of nano ZnO photocatalyst in a batch reactor is shown in Fig. 3. The condition for this study is pH = 7, weight of ZnO nanoparticles = 1 g/L, concentration = 50 ppm, temperature = 30 ± 0.1 °C. It is seen that in the presence of both UV light and ZnO nanoparticles, complete degradation done at an irradiation time of 1.5 h. But in the absence of UV light and in the presence ZnO nanoparticles, the phenol solution is stable though adsorption has been found to be responsible for the decrease in phenol concentration. For the same experiment performed in the absence of nano ZnO, only 0.5 % of phenol solution undergoes degradation when the UV lamp had been switched off and the reaction was allowed to occur in the darkness. Therefore these experiments demonstrated that both UV light and a photocatalyst were needed for the effective destruction of organic contaminant such as phenol in aqueous solution. It has been established that the photocatalyzed degradation of organic matter in solution is initiated by photo excitation of the semiconductor, followed by the formation of an electron-hole pair on the surface of nanophotocatalyst. The high oxidative potential of the hole (h^+VB) in the catalyst permits the direct oxidation of organic matter (phenol) to reactive intermediates[26]. Highly reactive hydroxyl radicals can also be formed either by the decomposition of water or by the reaction of the hole with OH^-. The hydroxyl radical is an

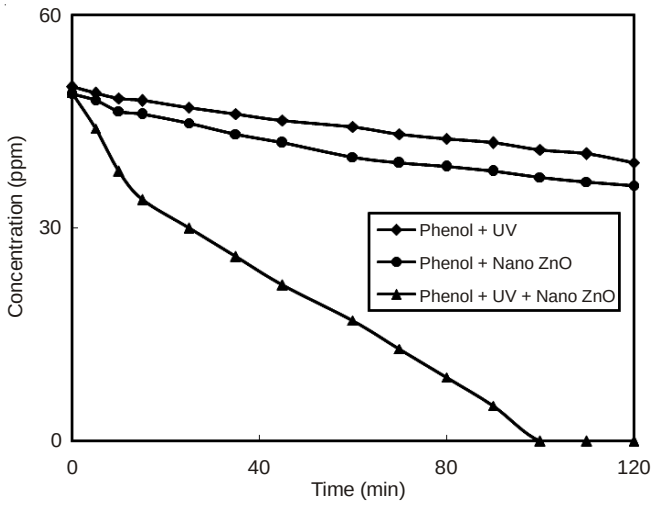

Fig. 3. Photodegradability of phenol; pH = 7.0; Weight of ZnO nanoparticles = 1 g/L; Concentration= 50 ppm; Incident wavelength = 254 nm; Temperature = 30 ± 0.1 °C

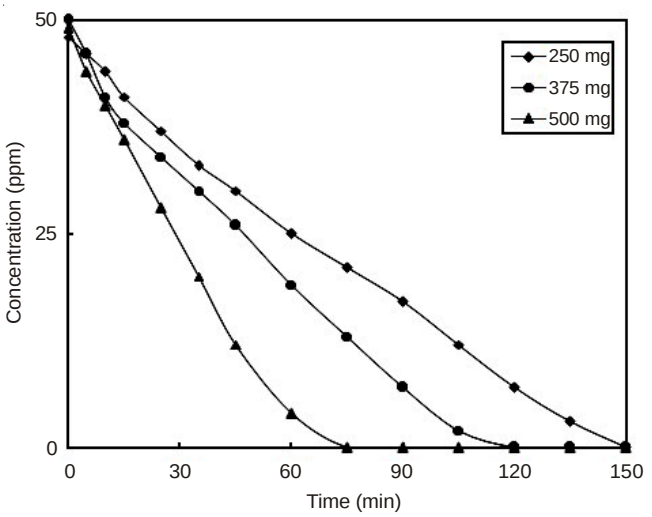

Fig. 4. Effect of catalyst weight on the photocatalytic degradation of phenol; pH = 7.0; Weight of ZnO nanoparticles = 1 g/L; Concentration= 50 ppm; Incident wavelength = 254 nm; Temperature = 30 ± 0.1 °C

extremely strong, non-selective oxidant ($E^0 = +3.06$ V) which leads to the partial or complete mineralization of several organic chemicals.

Effect of catalyst weight: Experiments performed with the effect of three different catalyst weights such as 1, 1.5 and 2 g/L is shown in the Fig. 4. It showed the photodegradation increased with an increase in the weight of the nanophotocatalyst. The effect of catalyst loading on the degradation of phenol in aqueous solution has been carried out at pH = 7, concentration = 50 ppm at room temperature. The catalyst weight 2 g/L shows higher photodegradation than 1 g/L and 1.5 g/L. The degradation process was quick and completed within 75 min. It is due to the fact that the total active surface area increases with increasing catalyst dosage (2 g/L). The catalyst concentration above which conversion levels off depends on several factors (*e.g.* reactor geometry, operating conditions, wavelength and intensity of light source) and corresponds to the point where all catalyst particles are fully illuminated[27]. There is domination of suspended ZnO nanoparticles due to excess load of catalyst comparing with 1 and 1.5 g/L. Additionally the rate of degradation increases with increase in catalyst loading from 0.5 to 1 g/L. It is important to keep the treatment expenses low for industrial use. So the optimum loading of 1 g/L was used for further investigation. In 1 g/L the degradation rate is normal and after 30th min it was quite fast and efficient and the complete reaction done within 150 min. And in 1.5 g/L the degradation process is faster, efficient and comparatively 1 g/L, it was completed at the 120th min.

The findings of this study have revealed that the photocatalytic rate initially increases with catalyst loading and then decreases at high values because of light scattering and screening effects. The tendency toward agglomeration (particle-particle interaction) also increases at high solids concentration, resulting in a reduction in surface area available for light absorption and hence a drop in photocatalytic degradation rate. Although the number of active sites in solution will increase with catalyst loading, a point appears to be reached where light penetration is compromised because of excessive particle concentration. The tradeoff between these two opposing phenomena results in an optimum catalyst loading for the photocatalytic reaction[28]. A further increase in catalyst loading beyond the optimum (1 g/L) will result in non-uniform light intensity distribution. So the reaction rate would indeed be lower with increased catalyst dosage. Selvam *et al.*[29] indicated that the degradation of 4-fluorophenol was done by the optimum concentration of 200 mg of ZnO and further increase in catalyst loading results in a decrease in the rate constant from 0.0358 to 0.0296 min^{-1}. Prabha and Lathasree[30] examined the effect of ZnO nanoparticles on the photocatalytic degradation of phenol in the range of 0.75-2.5 g/L. The optimum degradation was shown to be at 2 g/L ZnO nanoparticles under the experimental conditions. The decrease in the degradation rate beyond catalyst loading of 2 g/L was attributed to the screening effect of excess catalyst particles in the solution. Hong *et al.*[31] investigated the effect of catalyst dosage (1.0-4.0 g/L) on the photocatalytic degradation of phenol. Under the conditions tested, optimum degradation was achieved at 2 g/L. In order to ensure uniform light intensity in the photocatalytic reactor, optimum catalyst loading must be determined.

Effect of phenol concentration: Successful application of the photocatalytic degradation system requires the investigation of the dependence of photocatalytic degradation on the substrate (phenol) concentration. The effect of concentration of phenol in aqueous solution on photocatalytic degradation was carried out at fixed amount of the catalyst (1 g/L) and varying concentration of the phenol from 40-100 ppm is shown in Fig. 5. The photodegradation of phenol in aqueous solution decreases with an increase in the concentration of phenol. Parida and Parija[32] studied the effect of initial substrate concentration (2-25 g/L) on the photocatalytic degradation of phenol under UV light. Under UV light, the degradation was found to decrease from 94 to 52 % with increasing initial concentration. The degradation rate is directly proportional to the probability of formation of hydroxyl radicals ($OH^{\bullet}$) on the catalyst surface and the probability of hydroxyl radicals reacting with the phenol molecules[33]. As the concentration of the phenol

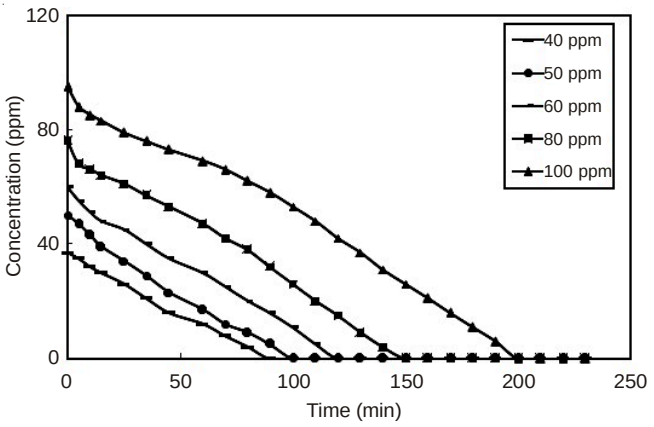

Fig. 5. Effect of concentration on the photocatalytic degradation of the phenol; pH = 7; Weight of ZnO nanoparticles = 1 g/L; Concentration= 50 ppm; Incident wavelength = 254 nm; Temperature = 30 ± 0.1 °C

in aqueous solution increases, there should be more interaction with $OH^{\bullet}$ radicals. At high phenol concentration the generation of $OH^{\bullet}$ radicals on the surface of catalyst is reduced since the active sites are covered with the phenol ions. Also, with increase in phenol concentration, less photons reach the photocatalyst surface (UV screening effect), resulting in slower production of hydroxyl radicals.

The concentration of target pollutant increases, more and more molecules of the compound get adsorbed on the surface of the photocatalyst. Therefore, the requirement of reactive species ($^{\bullet}OH$ and $^{\bullet}O^{2-}$) needed for the degradation of pollutant also increases. However, the formation of $^{\bullet}OH$ and $^{\bullet}O^{2-}$ on the catalyst surface remains constant for a given light intensity, catalyst amount and duration of irradiation. Hence, the available $^{\bullet}OH$ radicals are inadequate for the pollutant degradation at higher concentrations. Consequently the degradation rate of pollutant decreases as the concentration increases[34]. In addition, an increase in substrate concentration can lead to the generation of intermediates which may adsorb on the surface of the catalyst. Slow diffusion of the generated intermediates from the catalyst surface can result in the deactivation of active sites of the photocatalyst and consequently result in a reduction in the degradation rate.

The values of effect of concentration of phenol from 40-100 ppm in solar light degradation in the presence of ZnO nanoparticles is given in Table-2. Due to considerable wide concentration range of organic pollutants in factual wastewaters, it is needed to consider the effect of phenol solution in the presence of solar light. The degradation of phenol solution in the presence of ZnO nanoparticles is fast, efficient and completed from 90-195 min for 40-100 ppm of phenol solution as shown in Fig. 6. It is due to the fact that the degradation rate is directly proportional to the probability of formation of hydroxyl radicals ($OH^{\bullet}$) on the nano ZnO surface and the probability of hydroxyl radicals reacting with the phenol molecules[35]. At high concentration the generation of $OH^{\bullet}$ radicals on the surface of ZnO nanoparticles is reduced since the active sites are covered with phenolic ions. When the concentration of phenol increases, less photons reach the nano ZnO surface, resulting in slower production of hydroxyl radicals[36]. This is due to the reduction percentage of phenol in

TABLE-2
EFFECT OF CONCENTRATION ON THE PHOTOCATALYTIC DEGRADATION OF THE PHENOL IN SOLAR LIGHT

Time (min)	Phenol concentration (ppm) on irradiation at differential concentrations				
	40	50	60	80	100
Before adsorption	40	50	60	80	100
0	37	44	55	76	95
5	32	40	51	68	88
10	28	36	47	64	83
15	23	31	42	61	77
25	19	24	35	57	72
35	14	19	30	53	67
45	10	14	25	48	62
60	5	10	20	42	57
75	1	7	16	38	52
90	0	2	11	32	47
105	0	0	5	24	40
120	0	0	0	16	33
135	0	0	0	9	26
150	0	0	0	3	18
165	0	0	0	0	11
180	0	0	0	0	4
195	0	0	0	0	0
Initial rate (μM/m)	1±0.04	0.8±0.01	0.8±0.02	1.6±0.04	0.75±0.04

pH = 7.0; Weight of ZnO nanoparticles = 1 g/L; Concentration = 50 ppm; Absorbance measured at 500 nm

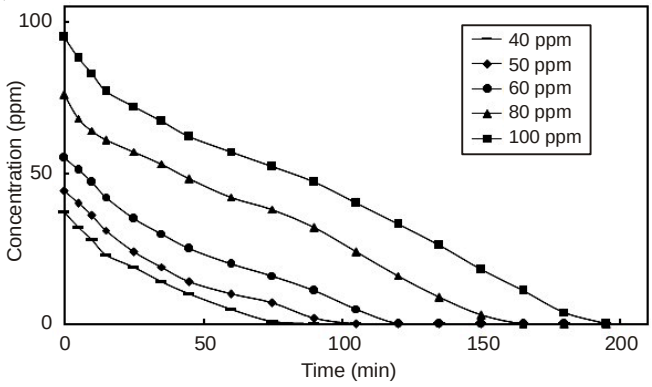

Fig. 6. Effect of concentration on the photocatalytic degradation of the phenol in solar light; Concentration = 50 ppm; pH = 7; Weight of ZnO nanoparticles = 1 g/L; Absorbance measured at 500 nm

aqueous solution and it depends strongly on the initial concentration of phenol in aqueous solution. As the initial concentration increases, more number of phenol molecules are adsorbed on the surface of ZnO nanoparticles until a saturated state occurs and there are fewer active sites for adsorption of hydroxyl ions, thereby reducing the generation of hydroxyl radicals. The highly oxidative holes on valence band of ZnO nanoparticles not only directly decompose the phenol molecules adsorbed on the surface of nanoparticles, but also oxidize H_2O or OH^- to form hydroxyl radicals ($^{\bullet}OH$) with high activity and indirectly degrade the phenol molecules in aqueous solution. These radicals can also degrade the surrounding organic phenol molecules, leading to volatile degradation by-products or entire mineralization into CO_2, H_2O and mineral acids. Through the degradation of phenol under solar light irradiation, ZnO nanoparticles shows promise in solar energy applications for the environmental cleanup.

TABLE-3
log C_0/C VALUE FOR THE CONCENTRATION OF PHENOL VARYING FROM 40-100 ppm

Time (min)	log C_0/C					k				
	40 ppm	50 ppm	60 ppm	80 ppm	100 ppm	40 ppm	50 ppm	60 ppm	80 ppm	100 ppm
0	–	–	–	–	–	–	–	–	–	–
5	0.1021	0.0399	0.0047	0.0082	0.0332	0.0470	0.0184	0.0021	0.0038	0.0152
10	0.2423	0.0787	0.0366	0.0256	0.028	0.0558	0.0181	0.0084	0.0059	0.0064
15	0.3383	0.1028	0.0545	0.0518	0.0386	0.0519	0.0158	0.0083	0.0079	0.0059
25	0.5456	0.3066	0.1562	0.0980	0.0700	0.1688	0.0282	0.0144	0.0091	0.0064
35	0.9702	0.4471	0.2236	0.1175	0.1012	0.0638	0.0294	0.0147	0.0077	0.0066
45	1.0293	0.7333	0.3245	0.2410	0.1244	0.0526	0.0375	0.0166	0.0123	0.0064

Kinetics studies on photocatalytic degradation of phenol: Under constant conditions of catalyst weight and photon flux the effect of concentration of the phenol solution on its photocatalytic degradability has been studied. The results show that the photocatalytic degradation of phenol solution follows pseudo first order kinetics. Ln (C_0/C) = kt, where C_0 is the initial concentration and C is the concentration at any time, t. Table-3 shows the ln C_0/C and k value for the concentration of phenol in aqueous solution varying from 40 to 100 μM. The plot of log (C_0/C) *vs.* t gave a straight line as shown in the Fig. 7. The correlation constant R^2 for the best fit line was calculated to be 0.999, 0.995, 0.997, 0.994 and 0.966 respectively. When the phenol in aqueous solution concentration increases, pseudo-first-order rate constant (k) decreases. This can be related to the decrease in the number of active sites on the catalyst surface, which is proportional to the initial concentration of phenol. Thus, the rate of hydroxyl radical generation on the catalyst surface will decrease, accordingly. Similar investigations have been reported for the photocatalytic oxidation of pollutants[37-40].

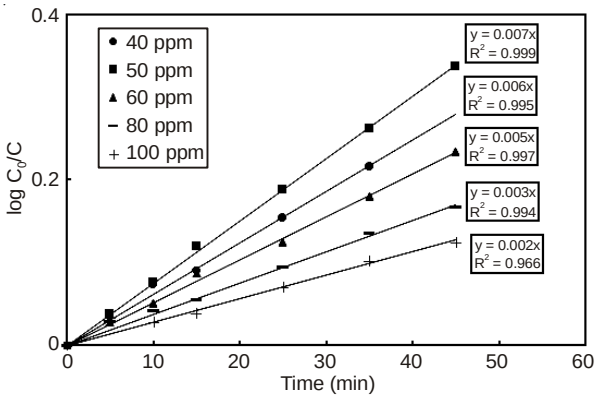

Fig. 7. Plot of C_0/C *versus* time for phenol; pH = 7; Weight of nano ZnO = 1 g/L; Concentration = 50 ppm; Incident wavelength = 254 nm; Absorbance measured at 500 nm; Temperature = 30 ± 0.1 °C

Addition of hydrogen peroxide: The photocatalytic degradation of phenol has been studied at different hydrogen peroxide concentrations (5-25 mmol/L). The photocatalytic degradation of organic pollutant as phenol depends upon their reactions with the •OH radicals. Therefore, the electron acceptors have been used to enhance the degradation rates since they generate •OH radicals[41]. By adding ZnO nanoparticles in the photoreactor, the photocatalytic degradation rate increased. In addition, the optimum concentration of H_2O_2 was investigated in the experiment series. In the absence of a suitable electron acceptor or donor, recombination step is predominant and thus, it limits the quantum yield. Thus, it is crucial to prevent the electron-hole recombination to ensure efficient photocatalysis. Hydrogen peroxide as an electron scavenger accepts a photo-generated electron from the conduction band and thus prevents electron-hole recombination forming •OH radicals. In addition, UV photons (from the radiation source) facilitate the decomposition of hydrogen peroxide, forming hydroxyl radicals[42]. The influence of hydrogen peroxide on the photocatalytic degradation of phenol is presented in Fig. 8. The degradation rate of phenol was increased with increasing H_2O_2 concentration up to 25 mM and thereafter decreases. This is because of the reaction of hydrogen peroxide with conduction band electrons and the superoxide radical anion to yield hydroxyl radicals and anions[43]. These reactions enhance the reactivity due to the formation of additional oxidizing species and also the suppression of e^-/h^+ recombination. Since hydrogen peroxide is a better electron acceptor than the molecular oxygen, it could act as an alternate for oxygen and hence enhances the degradation efficiency. When H_2O_2 is in excess, it acts as a powerful hydroxyl scavenger[44]. Thus it is clear that addition of optimal concentration of H_2O_2 shows a beneficial effect on the photocatalytic degradation of phenol.

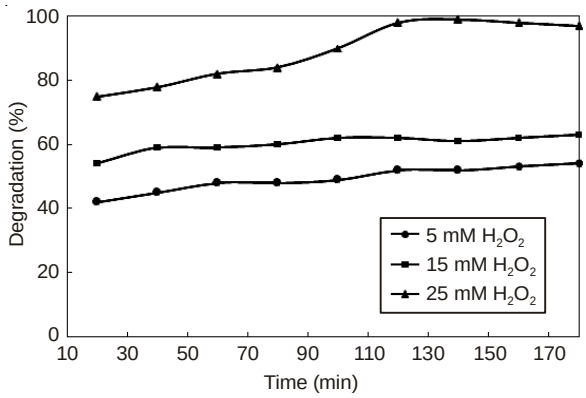

Fig. 8. Effect of H_2O_2 on the photodegradation efficiency of phenol; Weight of ZnO nanoparticles = 1 g/L; Incident wavelength = 254 nm; Absorbance measured at 500 nm; Concentration = 50 ppm; pH = 8.0; Irradiation time = 180 min; Temperature = 30 ± 0.1 ºC

Reusability of nanophotocatalyst: Reusability of ZnO nanoparticles for the photocatalytic degradation of phenol was evaluated. The nanocatalyst was separated from phenol solution by filtration, washed with water and dried at 100 and 200 °C.The dried ZnO nanoparticles were used for the degradation of phenol solution, employing under similar experimental conditions and procedures. Fig. 9 shows the reusability of ZnO nanoparticles at 100 °C. The results showed that the degradation extent decreases after four runs as 94, 86,

76 and 63 % for drying temperature of 100 °C. The decrease in the degradation percentage is explained by adsorption of organic intermediates and by-products of the photodegradation process in the cavities and on the surface of the photocatalyst that influences the surface activity of the nanocatalysts. Hence, for the dried catalysts at 200 °C, the decreasing of the degradation percentage is lower than the other trials. On the other hand, at higher temperature the excess of adsorbed molecules on the surface of the nanophotocatalysts was disappeared and the excess of degradation centers was released. Thus ZnO nanoparticles have higher effective surface. Also, in all the cases, the leached zinc cation into the solution decreases the semiconductor as the active sites on the nanocatalysts surface. This in turn reduces the photoreactivity of the remained catalysts in the photocatalytic process. In addition, in repetitive uses of the nanocatalysts, a loss was occurred in the amount of the reused nanophotocatalyst particles. The major advantage of the use of heterogeneous catalytic materials is their easy recovery. Unlike the homogeneous systems, these solid catalysts can be recuperated by means of a simple separation operation and reused in the next runs. In this sense, one of the principal goals of these types of processes is the development of stable heterogeneous catalysts with minimal leaching of active species under the reaction conditions. In many cases, catalysts have been reused giving reproducible and effective results.

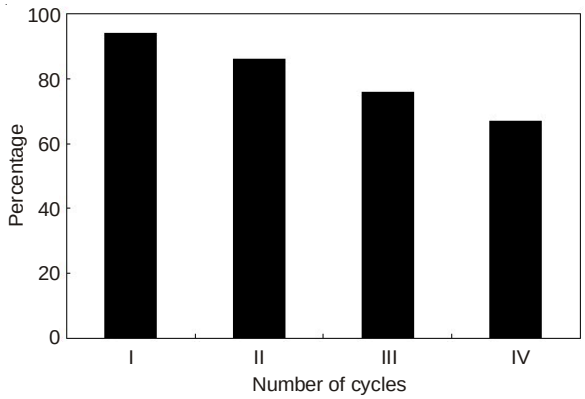

Fig. 9. Resuability of ZnO nanoparticles at 100 °C

Conclusion

Zinc oxide nanoparticles have been prepared successfully and confirmed by XRD pattern, SEM micrograph and BET surface area method. In conclusion, one of the industrial organic pollutant phenol was studied effectively for its photocatalytic degradation in UV and solar light in the presence of ZnO nanoparticles as the photocatalyst. The XRD data showed ZnO nanoparticles had Wurtzite structure with crystallite size as 35 ± 5 nm and SEM micrograph showed the heterogeneous and spherical shape of the nanoparticles with the particle size of 30 ± 5. The surface area was found to be 11.09 m^2/g. Introduced at comparatively lower dose, ZnO nanoparticle was found to be highly efficient in degrading the organic pollutant in wastewater. The photocatalytic degradation was improved with increasing amount of ZnO nanoparticles. From these evidences it is concluded that ZnO nanoparticles can be the efficient photocatalyst to handle the wastewater treatment problems to provide pollution free environment to the living beings. The photocatalytic degradation of phenol can be described with pseudo-first order reaction kinetics.

REFERENCES

1. S.H. Shin and D.S. Kim, *Environ. Sci. Technol.*, **35**, 3040 (2001).
2. J. Marchese, N.A. Ochoa, C. Pagliero and C. Almandoz, *Environ. Sci. Technol.*, **34**, 2990 (2000).
3. B. Zargar, H. Parham and A. Hatamie, *Chemosphere*, **76**, 554 (2009).
4. S.S. Patil and V.M. Shinde, *Environ. Sci. Technol.*, **22**, 1160 (1988).
5. Y.M. Slokar and A.M. Le Marechal, *Dyes Pigments*, **37**, 335 (1998).
6. U. Pagga and D. Brown, *Chemosphere*, **15**, 479 (1986).
7. A.T. Moore, A. Vira and S. Fogel, *Environ. Sci. Technol*., **23** 403 (1989).
8. J.M. Herrmann, *Catal. Today*, **53**, 115 (1999).
9. R.B.M. Bergamini, E.B. Azevedo and L.R.R. deAraujo, *Chem. Eng. J.*, **149**, 215 (2009).
10. K. Chiang, R. Amal and T. Tran, *J. Mol. Catal. Chem.*, **193**, 285 (2003).
11. P.B. Amama, K. Itoh and M. Murabayashi, *J. Mol. Catal. Chem.*, **217**, 109 (2004).
12. R.H. Horning, *Text. Chem. Color*, **9**, 24 (1997).
13. C.B. Almquist and P. Biswas, *J. Catal.*, **212**, 145 (2002).
14. J.C. Lee, M.S. Kim and B.-W. Kim, *Water Res.*, **36**, 1776 (2002).
15. A. Di Paola, E. Garcia-López, S. Ikeda, G. Marcì, B. Ohtani and L. Palmisano, *Catal. Today*, **78**, 87 (2002).
16. M.L. Curri, R. Comparelli, P.D. Cozzoli, G. Mascolo and A. Agostiano, *Mater. Sci. Eng.*, **23**, 285 (2003).
17. D.H. Yu, R.X. Cai and Z.H. Liu, *Spectrochim. Acta [A]*, **60**, 1617 (2004).
18. H.M. Lin, S.J. Tzeng, P.J. Hsiau and W.L. Tsai, *Nanostruct. Mater.*, **10**, 465 (1998).
19. Z.S. Hu, G. Oskam and P.C. Searson, *J. Colloid Interf. Sci.*, **263**, 454 (2003).
20. A.B. Djurisic, Y. Chan and E. Herbert Li, *Mater. Sci. Eng. B*, **38**, 237 (2002).
21. J.M. Herrmann, *Catal. Today*, **53**, 115 (1999).
22. J. Sato, H. Kobayashi, K. Ikarashi, N. Saito, H. Nishiyama and Y. Inoue, *J. Phys. Chem. B*, **108**, 4369 (2004).
23. H. Tian, J. Ma, X. Huang, L. Xie, Z. Zhao, J. Zhou, P. Wu, J. Dai, Y. Hu, Z. Zhu, H. Wang and H. Chen, *Mater. Lett.*, **59**, 3059 (2005).
24. M.B. Ettinger, C.C. Ruchhoft and R.J. Lishka, *Anal. Chem.*, **23**, 1783 (1951).
25. C. Hariharan, *Appl. Catal. A*, **304**, 55 (2006).
26. B. Su, K. Wang, N. Dong, H.M. Mu, Z.Q. Lei, Y.C. Tong and J. Bai, *J. Mater. Process. Technol.*, **209**, 4088 (2009).
27. C. Lung-Chyuan and C. Tse-Chuan, *J. Mol. Catal.*, **85**, 201 (1993).
28. A.A. Adesina, *Catal. Surv. Asia*, **8**, 265 (2004).
29. K. Selvam, M. Muruganandham, I. Muthuvel and M. Swaminathan, *Chem. Eng. J.*, **128**, 51 (2007).
30. I. Prabha and S. Lathasree, *Mater. Sci. Semicond. Process.*, **26**, 603 (2014).
31. S.S. Hong, C.S. Ju, C.G. Lim, B.H. Ahn, K.T. Lim and G.D. Lee, *J. Ind. Eng. Chem.*, **7**, 99 (2001).
32. K.M. Parida and S. Parija, *Sol. Energy*, **80**, 1048 (2006).
33. W.Z. Tang and H. An, *Chemosphere*, **31**, 4157 (1995).
34. W. Bahnemann, M. Muneer and M.M. Haque, *Catal. Today*, **124**, 133 (2007).
35. K.M. Parida and S. Parija, *Sol. Energy*, **80**, 1048 (2006).
36. K.M. Parida, S.S. Dash and D.P. Das, *J. Colloid Interf. Sci.*, **298**, 787 (2006).
37. A.A. Khodja, T. Sehili, J.F. Pilichowski and P. Boule, *Photochem. Photobiol. A: Chem.*, **141**, 231 (2001).
38. N.M. Mahmoodi and M. Arami, *Photochem. Photobiol. A: Chem.*, **182**, 60 (2006).
39. N.M. Mahmoodi, M. Arami and N.Y. Limaee, *J. Hazard. Mater.*, **133**, 113 (2006).
40. M. Nikazara, K. Gholivand and K. Mahanpoor, *Kinet. Catal.*, **48**, 214 (2007).
41. V. Sukharev and R. Kershaw, *J. Photochem. Photobiol. Chem.*, **98**, 165 (1996).
42. S.G. Yang, X. Quan, X.Y. Li, Y.Z. Liu, S. Chen and G.H. Chen, *Phys. Chem. Chem. Phys.*, **6**, 659 (2004).
43. N. San, A. Hatipoglu, G. Kocturk and Z. Cinar, *J. Photochem. Photobiol. Chem.*, **146**, 189 (2002).
44. E. Sanatgar-Delshade, A. Habibi-Yangjeh and M. Khodadadi-Moghaddam, *Monatsh. Chem.*, **142**, 119 (2011).